Sohag Journal of Mathematics
An International Journal

http://dx.doi.org/10.18576/sjm/110301

Two dimensional free surface flows over submerged obstacles

Abdelkader Laiadi[1,*] *and Abdelkrim Merzougui*[2]

[1]Department of Mathematics, Biskra University, Biskra, Algeria
[2]Department of Mathematics, M'sila University, M'sila, Algeria

Received: 19 Dec. 2023, Revised: 8 July. 2024, Accepted: 23 Jul. 2024
Published online: 1 Sep. 2024

Abstract: In this work, we study the problem of steady two-dimensional flows over multiple obstacles under the effects of gravity and surface tension in fluid of a constant depth, and in the presence of a uniform stream. The fluid is treated as inviscid and incompressible. The flow is assumed to be irrotational. The problem is solved numerically by using the boundary integral equation technique, based on Cauchy integral formula. It is shown that, for both supercritical and subcritical flows, solutions depend on three parameters: the Froude number F, the Weber number δ and the angles of obstacles γ and β. Finally, solution diagrams for all flow regimes are presented.

Keywords: Free surface flow, boundary integral equation, Weber number, Froude number.

1 Introduction

The problem of free surface fluid flow over obstacles has a long and well documented history. Many variations this problem can take have been used to model situations in engineering and atmospheric and oceanographic sciences. The simplest form the problem can take is when the flow consists of a single layer of inviscid, incompressible fluid flowing over an obstacle. However, in most cases, the specific geometry involved in the problem has been used to simplify the equations. Arbitrary bottom profiles are thus not generally permitted. For example, Forbes [3] and [4] considered flow of a single fluid layer over a semi-elliptical obstacle on the stream bed, and used conformal mapping to satisfy the bottom condition exactly. Forbes and Schwartz [5] considered flow over a semi-circular obstruction and Dias and Vanden-Broeck [6] studied the flow over a triangular weir. An exception is the work of King and Bloor [7] who in fact allowed an arbitrary bottom topography and a single layer of inviscid, incompressible fluid. A generalisation of the Schwarz-Christoffel transformation was used and the resulting integral and integro-differential equations were solved numerically. This paper is concerned with the numerical calculation of $2-$D fluid flow over a multiple obstacles. The flow is uniform far upstream. The effects of surface tension and the gravity are included in the boundary conditions and the problem is solved numerically by using the boundary integral equation. This equation expresses the hodograph variable on the boundary of the artificial plane. Numerically, this equation can be solved by discretizing the domain of integration to construct a system of nonlinear equations, and the Newton iteration method is applied. In presenting this paper, we organize the sections as follows. The problem is formulated in sect 2. The numerical procedure is described in sect 3 and the results are discussed in sect 4.

2 Mathematical formulation

We consider the steady two-dimensional flow of an inviscid and incompressible fluid over a multiple obstacles. The flow is assumed to be irrotational. Fluid domain is bounded below by a horizontal rigid wall xx', the two triangles $BCDEF$ by the angle γ, polygonal obstacle $GHLM$ by the angle β, where $0 < |\gamma| < \frac{\pi}{2}$ and $0 < |\beta| < \frac{\pi}{2}$, and above by the free surfaces KN (see Figure 1). Let us introduce Cartesian coordinates with the $x-$axis along the bottom and the $y-$ axis directed vertically upwards. As $x \longrightarrow \infty$, the flow is assumed to approach a uniform stream with constant velocity U and constant length H. It is convenient to define dimensionless variables by taking U as the unit velocity

* Corresponding author e-mail: laiadhi_a@yahoo.fr

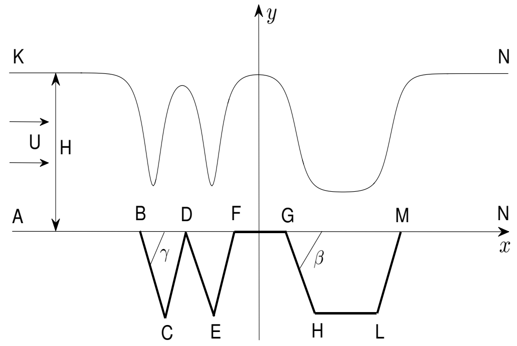

Fig. 1: Physical plane of the flow and of the coordinates. The figure is an actual computed profile for $F = 1.2$ and $\delta = 0.6$.

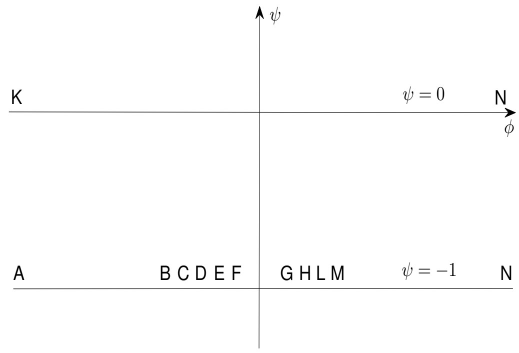

Fig. 2: The complex plane $f = \phi + i\psi$.

and H as the unit length. The dimensionless parameters in the problem are the Froude number

$$F = \frac{U}{\sqrt{gH}}$$

and the inverse Weber number

$$\delta = \frac{T}{\rho U^2 H}$$

and the dimensionless angles of obstacles γ and β. Here T is a surface tension, g is gravity and ρ is a fluid density. Let's introduce the velocity potential $\phi(x,y)$ and the stream function $\psi(x,y)$ by defining the complex potential function f as:

$$f(x,y) = \phi(x,y) + i\psi(x,y) \tag{1}$$

The complex velocity w can be written as:

$$w = \frac{df}{dz} = u - iv \tag{2}$$

Where u and v are the velocity components in the x and y directions and $z = x + iy$. We choose $\psi = 0$ along the free surface KN. The $\psi = -1$ and $-\infty < \phi < +\infty$ along the rigid bottom (see figure 2). The mathematical problem can be formulated in terms of the potential function ϕ satisfying the Laplace's equation

$$\Delta\phi = 0 \quad \text{in the fluid domain}$$

On the free surface, the Bernoulli equation has to be satisfied

$$\frac{1}{2}q^2 + \frac{p^*}{\rho} + g^* y^* = const = \frac{1}{2}U^2 + \frac{p_0}{\rho} + gH \tag{3}$$

where p^* is the fluid pressure, p_0 is the atmospheric pressure, ρ is the density, g^* is the gravitational constant and $q^2 = u^{*2} + v^{*2}$. It is noted that the right-hand-side of equation (3) is evaluated at the free surface far upstream. The Laplace's equation gives:

$$p^* - p_0 = \frac{T}{R} = KT \tag{4}$$

Where $K = \frac{1}{R}$ is the curvature. Substituting (4) into (3), and in terms of the dimensionless variables, Bernoulli's equation on the free surface becomes :

$$\frac{1}{2}\left(u^2 + v^2\right) + \delta K + \frac{1}{F^2}(y - 1) = \frac{1}{2} \tag{5}$$

The kinematic boundary conditions are

$$\begin{cases} v = 0 \text{ on } \psi = -1 \text{ and } -\infty < \phi < \phi_B \\ \text{and } \phi_M < \phi < +\infty \text{ and } \phi_F < \phi < \phi_G \\ v = u\tan|\gamma| \text{ on } \psi = -1 \text{ and } \phi_B < \phi < \phi_C \\ \text{and } \phi_D < \phi < \phi_E \\ v = u\tan|\beta| \text{ on } \psi = -1 \text{ and } \phi_G < \phi < \phi_H \\ \text{and } \phi_L < \phi < \phi_M \end{cases} \tag{6}$$

We now reformulate the problem as an integral equation. We define the function $\tau - i\theta$ by

$$w = u - iv = e^{\tau - i\theta} \tag{7}$$

and we map the flow domain onto the upper half of the $\zeta-$plane by the transformation

$$\zeta = \alpha + i\beta = e^{-\pi f} = e^{-\pi\phi}(\cos\pi\psi - i\sin\pi\psi) \tag{8}$$

The flow in the $\zeta-$plane is shown in figure 3. The velocity terms, first, become

$$u^2 + v^2 = e^{2\tau} \tag{9}$$

Secondly, the curvature K of a streamline, in terms of θ, is

$$K = -e^{\tau}\left|\frac{\partial\theta}{\partial\phi}\right| \tag{10}$$

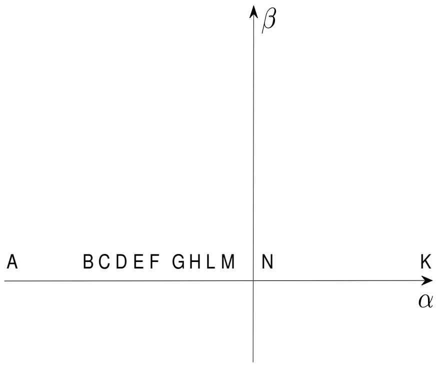

Fig. 3: The complex plane $\zeta = \alpha + i\beta$

Substituting (9) and (10) into (5), gives the final form of Bernoulli's equation that is needed for the numerical calculation. This is

$$\frac{1}{2}e^{2\tau} - \delta e^{\tau}\left|\frac{\partial\theta}{\partial\phi}\right| + \frac{1}{F^2}(y-1) = \frac{1}{2} \quad \text{on} \quad \text{KN} \qquad (11)$$

To construct an integral equation for this problem, we apply the Cauchy's integral formula to the function $\tau - i\theta$ in the complex $\zeta-$plane with a contour consisting of the real axis and the circumference of a half circle of arbitrary large radius in the upper half plane. After taking the real part, we obtain

$$\tau(\alpha_0) = -\frac{1}{\pi}\int_{-\infty}^{+\infty}\frac{\theta(\alpha)}{\alpha-\alpha_0}d\alpha \qquad (12)$$

Where $\tau(\alpha_0)$ and $\theta(\alpha)$ denote the value of τ and θ on the free surface. The kinematic boundary conditions (6) become

$$\begin{cases} \theta = 0 \quad -\infty < \alpha < \alpha_B \text{ and } \alpha_M < \alpha < 0 \\ \text{ and } \alpha_F < \alpha < \alpha_G \\ \theta = -\gamma \quad \alpha_B < \alpha < \alpha_C \text{ and } \alpha_D < \alpha < \alpha_E \\ \theta = \gamma \quad \alpha_C < \alpha < \alpha_D \text{ and } \alpha_E < \alpha < \alpha_F \\ \theta = -\beta \quad \alpha_G < \alpha < \alpha_H \\ \theta = \beta \quad \alpha_L < \alpha < \alpha_M \\ \theta = \text{ unknown } 0 < \alpha < +\infty \end{cases} \qquad (13)$$

Using (13), equation (12) become

$$\tau(\alpha_0) = J(\alpha_0) + U(\alpha_0) - \frac{1}{\pi}\int_0^{+\infty}\frac{\theta(\alpha)}{\alpha-\alpha_0}d\alpha \qquad (14)$$

Where

$$U(\alpha_0) = \frac{\beta}{\pi}\log\left|\frac{\alpha_H-\alpha_0}{\alpha_G-\alpha_0}\right| - \frac{\beta}{\pi}\log\left|\frac{\alpha_M-\alpha_0}{\alpha_L-\alpha_0}\right|$$

and

$$J(\alpha_0) = \frac{\gamma}{\pi}\log\left|\frac{(\alpha_C-\alpha_0)(\alpha_E-\alpha_0)}{(\alpha_B-\alpha_0)(\alpha_D-\alpha_0)}\right| - \frac{\gamma}{\pi}\log\left|\frac{(\alpha_D-\alpha_0)(\alpha_F-\alpha_0)}{(\alpha_C-\alpha_0)(\alpha_E-\alpha_0)}\right|$$

Equation (12) provides a relation between τ and θ on the free surfaces. Another relation between τ and θ on the free surface can be found from equation (11). Using (8) and integrating the identity

$$\frac{d(x+iy)}{df} = w^{-1} \qquad (15)$$

This gives

$$x(\alpha) = x_\infty - \frac{1}{\pi}\int_0^{\alpha}\frac{e^{-\tau(\alpha_0)}\cos\theta(\alpha_0)}{\alpha_0}d\alpha_0 \qquad (16)$$

for $0 < \alpha < +\infty$ and

$$y(\alpha) = 1 - \frac{1}{\pi}\int_0^{\alpha}\frac{e^{-\tau(\alpha_0)}\sin\theta(\alpha_0)}{\alpha_0}d\alpha_0 \qquad (17)$$

for $0 < \alpha < +\infty$.

By substituting (14) and (17) into (11), an integro-differential equation is created and this is solved numerically in the following section.

3 Numerical procedure

The above system of nonlinear equations is solved numerically by using equally spaced points in the potential function. Introducing the change of variables

$$\alpha = e^{-\pi\phi}$$

on free surface, we can rewrite (14) as

$$\tau'(\phi_0) = J'(\phi_0) + U'(\alpha_0) + \int_{-\infty}^{+\infty}\frac{\theta'(\phi)e^{-\pi\phi}}{e^{-\pi\phi}-e^{-\pi\phi_0}}d\phi \qquad (18)$$

Here

$$J'(\phi_0) = J\left(e^{-\pi\phi_0}\right) = \frac{\gamma}{\pi}\log\left|\frac{\left(e^{-\pi\phi_C}-e^{-\pi\phi_0}\right)\left(e^{-\pi\phi_E}-e^{-\pi\phi_0}\right)}{\left(e^{-\pi\phi_B}-e^{-\pi\phi_0}\right)\left(e^{-\pi\phi_D}-e^{-\pi\phi_0}\right)}\right| - \frac{\gamma}{\pi}\log\left|\frac{\left(e^{-\pi\phi_D}-e^{-\pi\phi_0}\right)\left(e^{-\pi\phi_F}-e^{-\pi\phi_0}\right)}{\left(e^{-\pi\phi_C}-e^{-\pi\phi_0}\right)\left(e^{-\pi\phi_E}-e^{-\pi\phi_0}\right)}\right|,$$

$$U'(\alpha_0) = \frac{\beta}{\pi}\log\left|\frac{e^{-\pi\phi_H}-e^{-\pi\phi_0}}{e^{-\pi\phi_G}-e^{-\pi\phi_0}}\right| - \frac{\beta}{\pi}\log\left|\frac{e^{-\pi\phi_M}-e^{-\pi\phi_0}}{e^{-\pi\phi_L}-e^{-\pi\phi_0}}\right|$$

and $\tau'(\phi_0) = \tau\left(e^{-\pi\phi_0}\right)$, $\theta'(\phi) = \theta\left(e^{-\pi\phi}\right)$. Accordingly, equations (11), (16) and (17) can be rewritten as follows

$$\frac{1}{2}e^{2\tau'(\phi_0)} - \delta e^{\tau'(\phi_0)}\left|\frac{\partial\theta'(\phi)}{\partial\phi}\right| + \frac{1}{F^2}(y'(\phi)-1) = \frac{1}{2} \qquad (19)$$

$$x'(\phi) = x_\infty + \int_{-\infty}^{\phi}e^{-\tau'(\phi_0)}\cos\theta'(\phi_0)d\phi_0 \qquad (20)$$

for $-\infty < \phi < +\infty$

$$y'(\phi) = 1 + \int_{-\infty}^{\phi} e^{-\tau'(\phi_0)} \sin\theta'(\phi_0) d\phi_0 \qquad (21)$$

for $-\infty < \phi < +\infty$.

Here $x'(\phi) = x\left(e^{-\pi\phi}\right)$, $y'(\phi) = y\left(e^{-\pi\phi}\right)$. Next we introduce equally spaced mesh points in the potential function by

$$\phi_I = \left[\frac{-(N-1)}{2} + (I-1)\right]\Delta, I = 1,...,N, -\infty < \phi < +\infty \qquad (22)$$

On the upstream and downstream free surfaces.

Here $\Delta > 0$. We evaluate the values τ' (ϕ_0) at the midpoints

$$\phi_M = \frac{\phi_{I+1} + \phi_I}{2}, I = 1,...,N-1 \qquad (23)$$

by applying the trapezoidal rule to the integral in (18) with summations over ϕ_I such that ϕ_0 is the midpoints. We evaluate $y_I = y'(\phi_I)$ by applying the trapezoidal rule and by using (20) and (21). This yields

$$\begin{cases} y_1 = 1 \\ y_{I+1} = y_I + \Delta e^{-\tau_M} \sin\theta_M, I = 1,...,N-1 \end{cases}$$

and

$$\begin{cases} x_1 = x_\infty \\ x_{I+1} = x_I + \Delta e^{-\tau_M} \cos\theta_M, I = 1,...,N-1 \end{cases}$$

Here $\theta_M = \dfrac{\theta_{I+1} + \theta_I}{2}$. We now satisfy (19) at the midpoints (23). This yields N nonlinear algebraic equations for the N unknowns $\theta_I, I = 1,...,N$. The derivative, $\dfrac{\partial\theta'}{\partial\phi}$, at the mesh points (22), is approximated by a finite difference, whereby

$$\frac{\partial\theta'}{\partial\phi} \approx= \frac{\theta_{I+1} - \theta_I}{\Delta}, I = 1,...,N-1$$

For a given values of δ, γ, β and F, this system of N equations with N unknowns is solved by Newton's method.

4 Results and discussion

We found that there is a three-parameters family of solutions. The three parameters can be chosen as the Froude number F, δ and the values of γ and β. The numerical procedure of section 3 was used to compute supercritical $(F > 1)$ and subcritical $(F < 1)$ solutions. These flows are symmetrical with respect to the $y-$ axis and do not contain waves. Most of the calculations are obtained with $N = 401$ and $\Delta = 0.15$. Figures 4-7 show the effects of the two parameters Froude number F and inverse Weber number δ on the shape of the free-surface profiles for given values of the angles γ and β. A comparison of free surface profiles for various values of the inverse Weber δ are shown in the figures 6 and 7. It is found that the elevation of the free-surface falls down by the increases of the inverse Weber δ. The shape of a non linear free surface profiles for a symmetric solution of sub critical flow is shown in the figure 4. For supercritical flows as shown in figure 5. Figure 8 shows the shape of free-surfaces for different values of the angle β.

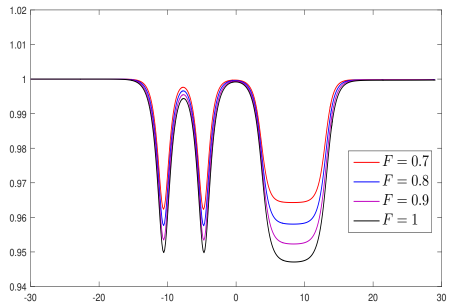

Fig. 4: Profiles of the free surfaces when $\delta = 1$ and $\gamma = \beta = -\frac{\pi}{3}$ and various values of Froude number F.

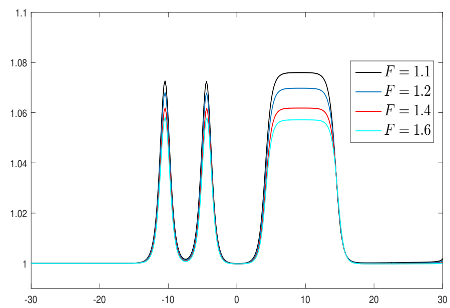

Fig. 5: Profiles of the free surfaces when $\gamma = \beta = \frac{\pi}{4}$ and various values of Froude number F.

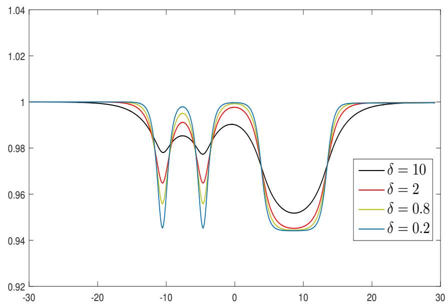

Fig. 6: Profiles of the free surfaces when $F \to \infty$ and $\gamma = \beta = -\frac{\pi}{4}$ and various values of Weber number δ.

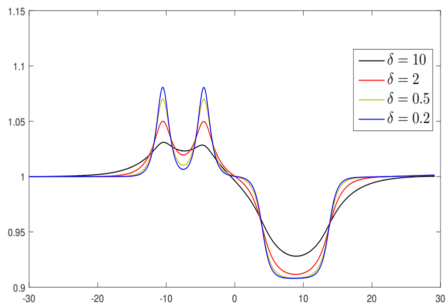

Fig. 7: Profiles of the free surfaces when $F = 1.2$ and $\gamma = \frac{\pi}{4}$ and $\beta = -\frac{\pi}{4}$ and various values of Weber number δ.

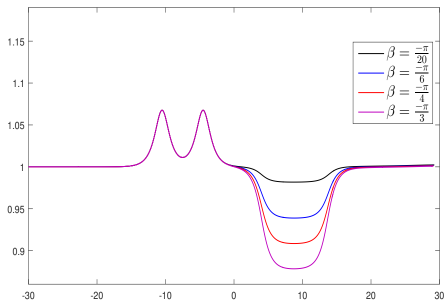

Fig. 8: Shape of free surfaces for $F = 1.2$, $\delta = 0.6$ and $\gamma = \frac{\pi}{4}$ and various values of the angle β.

References

[1] R. J. Holmes and G. C. Hoking, A note on waveless subcritical flow past symmetric bottom topography, Euro . Jnl of Applied Mathematics, **28**, 562-575 (2017).

[2] Sarwat N. Hanna, Influence of surface tension on free surface flow over a polygonal and curved obstruction, Journal of Computational and Applied Mathematics, **51**, 357-374 (1994).

[3] L. K. Forbes, On the wave resistance of a submerged semi-elliptical body, J. Eng. Math, **15**, 287-298 (1981).

[4] A. Merzougui and A. Laiadi, Free surface flow over a triangular depression, TWMS. J. App. Eng. Math, **4**, No(1), 67-73 (2014).

[5] L. K. Forbes and L. W. Schwartz, Free surface flow over a semi-circular obstruction, J. Fluid. Mech, **114**, 299- 314 (1982).

[6] F. Dias and J. M. Vanden-Broeck, Open channel flows with submerged obstructions, J. Fluid. Mech, **206**, 155- 170 (1989).

[7] A. C. King, and M. I. G. Bloor, Free surface flow of a stream obstructed by an arbitrary bed topography, Quart. J. Mech. Appl. Math, **43**, 87-106 (1990).

[8] L. K. Forbes, Free-surface flow over a semi-circular obstruction including the influence of gravity and surface tension, J. Fluid. Mech, **127**, 283-297 (1983).

[9] J. M. Vanden-Broeck, Numerical calculations of the free surface flow under a sluice gate, J. Fluid. Mech, **330**, 339-347 (1997).

[10] S. R. Belward and L. K. Forbes, Nonlinear two-layer flow over arbitrary topography, J. Eng. Math, **27**, 419-432 (1993).